

OPTICAL REMOTE SENSING OF THE BIOSPHERE WITH THE HELP OF MULTISPECTRAL AEROSPACE IMAGES

V.V. Kozoderov and V.S. Kosolapov

Institute of Computer Mathematics of the Russian Academy of Sciences, Moscow

Received April 20, 1992.

A new technique is proposed for estimating the soil and vegetation parameters from multispectral airborne and satellite data. The technique is based on improved concept of the soil brightness and of the quality index of green color of vegetation as well as on the models of interaction of the optical radiation with the atmosphere and earth's surface. Some examples of a relationship between the biomass of vegetation and satellite data are presented.

INTRODUCTION

Experience in investigation of the Earth from space in the 1980's has shown that for the problem of global variations the data of satellite scanning radiometers obtained with low spatial resolution (of the order of 1 km), which can yield routine information about the "ground-atmosphere" system several times a day all over the globe,¹ are most promising. The advantages of the systems with the above-indicated temporal resolution have been demonstrated over the systems with high spatial resolution (several tens of meters) which are used as an auxiliary means for thematic interpretation of images obtained in the visible and infrared (IR) regions of spectrum. Such an application of these systems is due to their small viewing swath at the moment of imaging and for this reason the repeated imaging of the same regions can be performed only in two or three weeks, and in practice (due to illumination conditions, cloudiness, etc.) in several months. All this leads to impossibility of their use, for example, for monitoring of the dynamics of vegetation growth and soil moistening.

It has been shown that the multispectral character of corresponding measurements aids in using the above-mentioned systems of both types in investigations of the biosphere, in which the atmosphere interferes with processing, interpretation, and subsequent estimate of the parameters describing the dry land state from the data of remote optical sensing. Fundamental progress in this area is associated with the evidence of the relations between the normalized vegetation indices (NDVI), which are widely used in practice and represent some combinations of measuring channels of scanning radiometers, active photosynthetically absorbed radiation (PAR), and primary productivity of vegetation (the rate of change of the amount of phytomass over vegetative period).² The concept of the B, G coordinates³ consisting in obtaining the other combinations of measuring channels of the type "soil brightness" (B) and "quality index of green color of vegetation" (G) is alternative to some extent to the concept of vegetation indices. It makes it possible to attach the results of multispectral satellite measurements to airborne and ground-based spectral radiometric and biophysical measurements, thereby providing the basis for foundation of the composition of hardware required to perform the integrated subsatellite experiments.⁴

We will discuss the advantage of the second concept which provides well-grounded acquisition and systematization of the *a priori*, reference, and other data needed for objective qualitative estimate of the states of vegetation and soil.⁵

MODELING OF REFLECTIVE PROPERTIES OF VEGETATION AND SOILS

At present the measurements in individual spectral channels of visible and near-infrared (IR) spectral regions are being most widely used in investigation of biosphere with the help of aerospace apparatus. As an example, Fig. 1 shows the spectral sensitivity $R(\lambda)$ (λ is the wavelength of measurements) of an AVHRR radiometer and MSS apparatus used onboard the NOAA and LANDSAT (USA). The three-channel MSU-E apparatus (with a spatial resolution of 45 m) used onboard the Soviet satellite "Kosmos-1939" is, to some extent, an analog of the MSS apparatus. The above-mentioned types of apparatus are used below to illustrate the results obtained by the new method for estimating the parameters of vegetation and soils from the multispectral aerospace images.

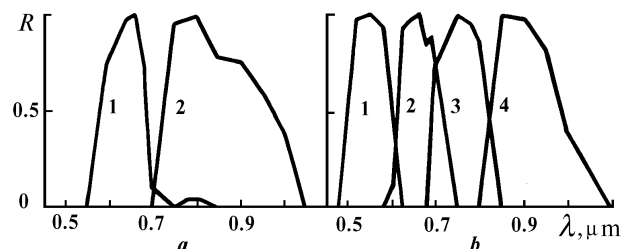


FIG. 1. Spectral channels of the AVHRR (a) and MSS (b) apparatus.

The outgoing radiation in the most general case of the i th object being measured in the j th channel of measuring apparatus of the k th type near the ground can be written down in the following form:

$$L_j(i, n, k, r, M, \theta, \varphi, h_\odot) = \frac{1}{2\pi^2} \int_0^{2\pi} \int_0^{\pi/2} \int_{\lambda_1}^{\lambda_2} [E_s(n, \lambda, h_\odot, \varphi') + H_s(n, \lambda, h_\odot, \theta', \varphi')] \rho_i(\lambda, r, M, \theta, \varphi, \theta', \varphi') R_j(k, \lambda, \Omega) \times \cos \theta' d\lambda d\theta' d\varphi', \quad (1)$$

where $E_s(n, \lambda, h_\odot, \varphi')$ is the direct solar radiation near the ground; $H_s(n, \lambda, h_\odot, \theta', \varphi')$ is the scattered solar radiation near the ground; h_\odot is the solar zenith angle; n is the type of the atmosphere (see below) which is determined by the transparency P and brightness of the atmospheric haze D

($1 \leq n \leq 4$); $\rho_i(\lambda, r, M, \theta, \varphi, \theta', \varphi')$ is the function of bidirectional reflection (phase function of reflection); M is the biomass of vegetation (t/ha); θ and φ are the zenith and azimuthal viewing angles, respectively; θ' and φ' are the same angles of the radiation incident on the ground; r is the soil parameter taking into account the type, moisture content, and state of the surface soil; $R_j(k, \lambda, \Omega)$ is the spectral sensitivity (instrumental function) of the apparatus in the corresponding channel in the wavelength range from λ_1 to λ_2 with the spatial resolution determined by the field-of-view angle Ω . The subscript i , as a rule, is further dropped. It can be seen from Eq. (1) that the angular distribution of the intensity of reflected radiation is a function of physical properties and state of the reflecting surface as well as of the conditions of illumination of the surface by the incident radiation. The illumination conditions are determined primarily by the solar zenith angle (h_\odot), atmospheric transparency, and cloudiness. Thus, the intensity of radiation reflected from the given surface is the function of the angles of incidence of illuminating radiation θ' and of reflection θ as well as of the difference between the azimuthal angles of incident and reflected radiations. All of them determine the function $\rho_i(\dots, \theta, \varphi, \theta', \varphi')$ called the phase function of reflection from the surface (or the bidirectional function of reflection).

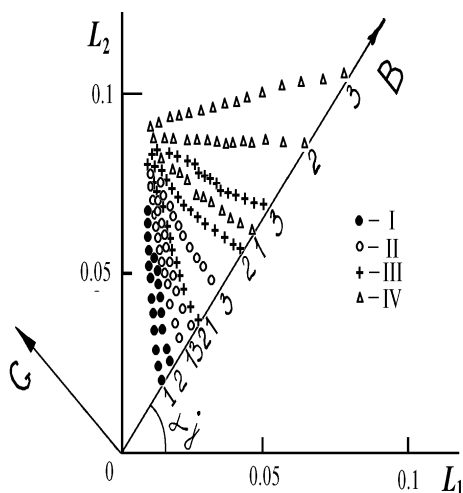


FIG. 2. Results of airborne measurements of the quantities L_1 and L_2 in the second and fourth channels of the MSS obtained for vegetation (winter wheat) with the amount of phytomass M varying from 0 (along the B axis) to 30 t/ha (region of condensation of points) for various soil types: chernozem (I), dark chestnut-colored soils (II), sod-podzolic soils (III), and sierozem (IV); 1) aqueous soils, 2) soils with 50 % moistening, and 3) dry soils. B, G is the new coordinate system, α_j is the angle of its rotation about the axes L_1 and L_2 .

As a rule, in the practical applications the values of L are scaled to a certain effective large amount of radiation, for example, to the brightness of the direct incident solar radiation in the corresponding channel of measuring apparatus (i. e., we measure $L_{1,2}$ in the fractions of solar brightness)

$$\hat{L}_1(i, n, k, r, M, \theta, \varphi, h_\odot) = \frac{L_1(i, n, k, r, M, \theta, \varphi, h_\odot)}{L_1^\odot(k)},$$

$$\hat{L}_2(i, n, k, r, M, \theta, \varphi, h_\odot) = \frac{L_2(i, n, k, r, M, \theta, \varphi, h_\odot)}{L_2^\odot(k)}, \quad (2)$$

where $L_{1,2}^\odot(k) = \int_{\lambda_1}^{\lambda_2} E_s^\downarrow(\lambda) R_j(k, \lambda, \Omega) d\lambda$ and $E_s^\downarrow(\lambda)$ is the

direct solar radiation incident on the top of the atmosphere (measured at the satellite orbit altitude). For simplicity we further drop the symbol of normalization atop L as well as its dependence on all the above-mentioned parameters.

The objects of soil-vegetative cover observed in different measuring channels of apparatus used onboard the satellite or aircraft and their images in the coordinates L_1 and L_2 may be classified as "soil line" or "vegetation line" (Fig. 2).

In the first case the spread of points indicates the change from dark soils (moisten soils or soils with large amount of humus) to light, dry, and less fertile soils. In the second case the change can be seen from sparse vegetation to dense bright-green vegetation with large amount of phytomass. In such a way the concept has arisen of analyzing the spaceborne imaging of soil-vegetative cover in the coordinates "soil brightness" B (brightness) – "quality index of green color of vegetation" G (greenness) which make it possible to divide the individual elements of satellite images into such classes as "soil", "normal vegetation" and "vegetation in stress state". The quantities B and G represent the linear combinations of outgoing radiation (L_1, L_2) in the measuring channels (x_1, x_2) and in the case of ground-based measurements this relation has the simplest form

$$B(n, k, r, M, \theta, \varphi, h_\odot) = a_1^b(n, k, r, \theta, \varphi, h_\odot) L_1 + a_2^b(n, k, r, \theta, \varphi, h_\odot) L_2;$$

$$G(n, k, r, M, \theta, \varphi, h_\odot) = a_1^g(n, k, r, \theta, \varphi, h_\odot) L_1 + a_2^g(n, k, r, \theta, \varphi, h_\odot) L_2, \quad (3)$$

where $a_{1,2}^{b,g}(n, k, r, \theta, \varphi, h_\odot)$ are the coefficients of conversion from "old" (L_1, L_2) to "new" (B, G) orthogonal system by means of the left rotation of coordinate axes (L_1, L_2) at the angle $\alpha_j = \arccos a_1^b(n, k, \theta, \varphi, h_\odot)$. These coefficients are determined by the least-squares method: at first the slope tangent ($\tan z$) of the regression straight line for the set of "soil points" without vegetation ($M = 0$) is determined and then the new coordinate system (B, G) is assigned by means of the left rotation of the old coordinate system (L_1, L_2) at the angle $\alpha_j = \arctan z$. Corresponding rotation coefficients have the form

$$a_1^b(n, k, \dots, h_\odot) = \cos \alpha_j, \quad a_2^b(n, \dots, h_\odot) = \sin \alpha_j,$$

$$a_1^g(n, \dots, h_\odot) = -\sin \alpha_j, \quad a_2^g(n, \dots, h_\odot) = \cos \alpha_j. \quad (4)$$

The above-indicated conversions are illustrated by Fig. 2. If the coordinate B is chosen in the direction of increasing the soil brightness corresponding to zero phytomass of plant canopies, another (normal to the soil axis) coordinate axis can be traced in the direction of increasing the quality index of green color G determining the growth of the ground phytomass of vegetation. The data shown in Fig. 2 are based on the results of airborne spectrometric measurements performed for different amount of the phytomass M (wheat) varying from 1 to 30 t/ha for observation in the nadir.⁶ It can be seen from Fig. 2 that with increase of M all measurement points merge into one class of "continuous plant canopies". It is evident that the intermediate state of vegetation between the "soil class" and "continuous plant canopies" in a number of cases can be considered as "vegetation in the stress state".

DISTORTING EFFECT OF THE ATMOSPHERE

Here we consider the simplest model of the effect of the atmosphere on the transformation of radiation reflected by the soil—vegetation system.

For radiation L_j^* received onboard the satellite we will employ the simplest model of its relation to L_j measured near the ground in the form

$$\left. \begin{aligned} L_1^* &= L_1 P_1(n, k, \theta) + D_1(n, k, \theta) \\ L_2^* &= L_2 P_2(n, k, \theta) + D_2(n, k, \theta) \end{aligned} \right\} \quad (5)$$

where $P_{1,2}(n, k, \theta)$ and $D_{1,2}(n, k, \theta)$ are the atmospheric transparency and the brightness of the atmospheric haze in the channels 1 and 2, respectively (1 is the short-wave channel and 2 is the long-wave channel). If necessary, the exact expressions for both quantities can be written down within the framework of the radiation transfer theory.⁷ Using these relations as well as Eq. (3) we obtain

$$\begin{aligned} B(n, k, r, M, \theta, \varphi, h_\odot) &= \frac{a_1^b(n, \dots, h_\odot)}{P_1(n, k, \theta)} L_1^* + \\ &+ \frac{a_2^b(n, \dots, h_\odot)}{P_2(n, k, \theta)} L_2^* - \left(\frac{a_1^b(n, \dots, h_\odot)}{P_1(n, k, \theta)} D_1(n, k, \theta) + \right. \\ &+ \left. \frac{a_2^b(n, \dots, h_\odot)}{P_2(n, k, \theta)} D_2(n, k, \theta) \right); \\ G(n, k, r, M, \theta, \varphi, h_\odot) &= \frac{a_1^g(n, \dots, h_\odot)}{P_1(n, k, \theta)} L_1^* + \\ &+ \frac{a_2^g(n, \dots, h_\odot)}{P_2(n, k, \theta)} L_2^* - \left(\frac{a_1^g(n, \dots, h_\odot)}{P_1(n, k, \theta)} D_1(n, k, \theta) + \right. \\ &+ \left. \frac{a_2^g(n, \dots, h_\odot)}{P_2(n, k, \theta)} D_2(n, k, \theta) \right). \end{aligned} \quad (6)$$

If in analogy with Eq. (3) for the brightness and the quality index of green color measured from onboard the satellite we assume that

$$\begin{aligned} B^*(n, k, r, M, \theta, \varphi, h_\odot) &= a_1^{*b}(n, \dots, h_\odot) L_1^* + a_2^{*b}(n, \dots, h_\odot) L_2^*; \\ G^*(n, k, r, M, \theta, \varphi, h_\odot) &= a_1^{*g}(n, \dots, h_\odot) L_1^* + a_2^{*g}(n, \dots, h_\odot) L_2^* \end{aligned} \quad (7)$$

then using Eq. (6) we can relate "old" (at the ground level) and "new" (at the satellite orbit altitude) values of the brightness and quality index of green color as follows:

$$\begin{aligned} B(n, \dots, h_\odot) &= B^*(n, \dots, h_\odot) - \Delta B_D(n, \dots, h_\odot); \\ G(n, \dots, h_\odot) &= G^*(n, \dots, h_\odot) - \Delta G_D(n, \dots, h_\odot), \end{aligned} \quad (8)$$

where $\Delta B_D(n, \dots, h_\odot)$ and $\Delta G_D(n, \dots, h_\odot)$ are the corrections for the effect of the atmosphere (in Eq. (6) these corrections are put in parentheses) which are the functions of the atmospheric haze brightness, while the relation between "new" and "old" coefficients is evident

$$a_1^{*b}(n, \dots, h_\odot) = \frac{a_1^b(n, \dots, h_\odot)}{P_1(n, k, \theta)},$$

$$a_2^{*b}(n, \dots, h_\odot) = \frac{a_2^b(n, \dots, h_\odot)}{P_2(n, k, \theta)};$$

$$a_1^{*g}(n, \dots, h_\odot) = \frac{a_1^g(n, \dots, h_\odot)}{P_1(n, k, \theta)},$$

$$a_2^{*g}(n, \dots, h_\odot) = \frac{a_2^g(n, \dots, h_\odot)}{P_2(n, k, \theta)}. \quad (9)$$

If for each class of vegetation the complete information was available, that is, for the various solar zenith angles h_\odot and various types of vegetation and amount of their biomass M their phase functions of reflection $\rho_i(\lambda, r, M, \theta, \varphi, \theta', \varphi')$ and the angular distribution of direct and scattered solar radiations were known, the coefficients $a_{1,2}^{*b,g}$ as well as B, G characteristics would be calculated successively on account of their angular anisotropy from the above formulas.

Unfortunately, at present we have no systematized data on the phase functions of reflection for different plant crops.

However, based on the well-known data (Refs. 6 and 8) we may conclude that under certain observation conditions at the solar zenith angles $h_\odot \geq 30^\circ$ and at the viewing angles up to $25-30^\circ$ as well as at the azimuthal viewing angles φ lying in the planes being far from the plane of solar vertical, i. e., at φ near 90° and 270° , the anisotropy of reflection of the soil—vegetation system in the visible and near-IR spectral ranges is small (less than 15%) and in the first approximation the angular dependence of reflective properties of the soil—vegetation system can be ignored.

Now, restricting ourselves to the conditions of relatively isotropic (Lambertian) vegetation surfaces (given that the above-indicated conditions are satisfied), we have for the outgoing radiation near the object

$$\begin{aligned} L_j(n, k, r, M, h_\odot) &= \frac{1}{\pi} \int_{\lambda_1}^{\lambda_2} [E_s(n, \lambda, h_\odot) + H_s(\lambda, h_\odot)] \times \\ &\times \rho_i(n, \lambda, r, M) R_j(k, \lambda, \Omega) d\lambda. \end{aligned} \quad (1')$$

Hereafter we will follow the above-considered approach which includes scaling of $L_{1,2}$ to the brightness of direct incident solar radiation, finding of the values of $L_{1,2}^*$ distorted by the atmosphere, and so on.

TABLE I. Atmospheric transparency and brightness of the atmospheric haze ($W/m^2 \cdot sr$) for four states of the atmosphere and the MSS apparatus for observation in the nadir.

Parameter	MSS, the second and fourth channels				MSS, the first and third channels			
	a	b	c	d	a	b	c	d
D_1	1.90	1.35	0.95	0.65	4.00	2.90	2.10	1.50
D_2	1.60	1.15	0.80	0.55	1.30	0.90	0.65	0.45
P_1	0.78	0.82	0.86	0.89	0.71	0.75	0.80	0.85
P_2	0.86	0.89	0.92	0.96	0.82	0.86	0.89	0.93

The problem of evaluation of the effect of the atmosphere on the satellite images is simplified owing to the relation between the quantities $P_{1,2}$ and $D_{1,2}$. For this reason the "type of the atmosphere" characteristic n can be employed

instead of the two-parametric family (P, D). For example, four types of possible combinations of the quantities $P_{1,2}$ and $D_{1,2}$ (for the observations in the nadir direction ($\theta = 0^\circ$)) and the MSS apparatus, which apparently cover the entire range of atmospheric states often encountered and correspond to the following conditions of atmospheric turbidity: strong (a and b), moderate (b), and weak (c) turbidities, are listed in Table I.

When viewing at the angle θ the relation of $P_{1,2}$ and $D_{1,2}$ to their values for observation in the nadir has the form

$$P_{1,2}(\theta)P_{1,2}(0)^{m(\theta)}, D_{1,2}(\theta) = D_{1,2}(0) + \frac{\partial D_{1,2}(0)}{\partial P_{1,2}}(P(\theta) - P(0)),$$

where $m(\theta)$ is the optical mass of the atmosphere.

The coefficients $a_{1,2}^{*b,g}$ converting the quantities L_1^* and L_2^* , measured with the help of second and fourth channels of the MSS apparatus, into the coordinates B^* and G^* for the four above-mentioned atmospheric states at the indicated angles θ and h_\odot are given in Table II.

TABLE II. The coefficients $a_{1,2}^{*b,g}$ of conversion of the quantities L_1^* and L_2^* , measured from onboard the satellite with the help of the second and fourth channels of the MSS apparatus for different states of the atmosphere at the indicated angles θ and h_\odot .

θ	Coefficients	h_\odot							
		70°				33°			
0°	a_1^{*b}	0.741	0.720	0.698	0.675	0.796	0.749	0.720	0.693
	a_2^{*b}	0.955	0.910	0.867	0.833	0.917	0.890	0.852	0.820
	a_1^{*g}	-1.046	-0.994	-0.938	-0.898	-1.005	-0.972	-0.922	-0.885
	a_2^{*g}	0.676	0.659	0.645	0.626	0.726	0.686	0.665	0.642
15°	a_1^{*b}	0.759	0.734	0.709	0.683	0.816	0.765	0.731	0.701
	a_2^{*b}	0.970	0.921	0.874	0.836	0.931	0.900	0.859	0.824
	a_1^{*g}	-1.073	-1.014	-0.953	-0.909	-1.030	-0.922	-0.936	-0.895
	a_2^{*g}	0.686	0.667	0.651	0.628	0.738	0.694	0.670	0.645

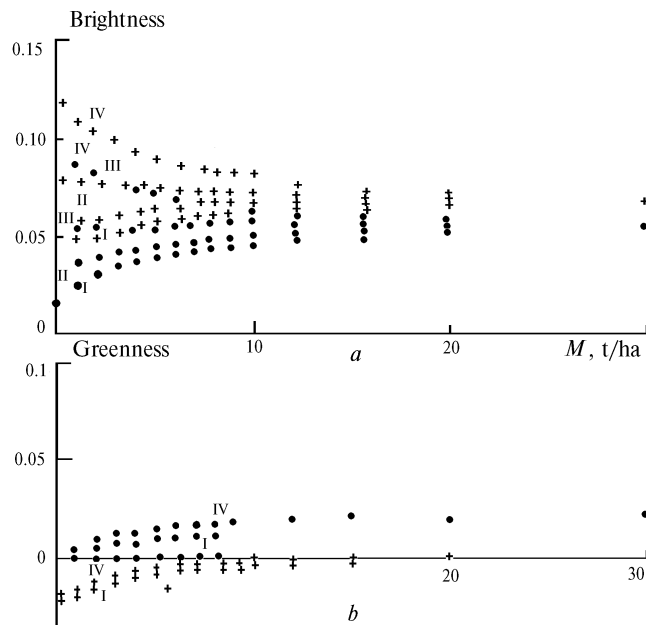


FIG. 3. Dependence of the soil brightness (a) and the quality index of green color (b) on the vegetation biomass according to the data of Ref. 6 near the ground (dots) and at the top of strongly turbid (a) atmosphere (crosses). The first and third channels of the MSS apparatus. Roman numbers denote the soil types indicated in Fig. 2.

REFERENCES

1. G. Asrar, *Theory and Application of Optical Remote Sensing* (John Wiley and Sons, New York, 1989), 890 pp.
2. S.D. Prince and C.O. Justice, *Int. J. Remote Sens.*, No. 12, 1133–1422 (1991).
3. R.C. Cicone and M.D. Metzler, *Remote Sens. Environ.*, No. 14, 257–265 (1984).
4. K.Ya. Kondrat'ev, V.V. Kozoderov, P.P. Fedchenko, and A.G. Topchiev, *Biosphere: Methods and Results of Remote Sensing* (Nauka, Moscow, 1990), 224 pp.
5. V.V. Kozoderov, in: *Fundamental Sciences to the National Economy* (Nauka, Moscow, 1990), pp. 13–16.
6. V.I. Rachkulik and M.V. Sitnikova, *Reflectivity and State of Plant Canopies* (Gidrometeoizdat, Leningrad, 1981), 288 pp.
7. P.J. Curran, G.M. Foody, K.Ya. Kondrat'ev, V.V. Kozoderov, and P.P. Fedchenko, *Remote Sensing of Soils and Vegetation in the USSR* (Taylor and Francis, London, 1990), 203 pp.
8. K.Ya. Kondrat'ev, V.I. Binenko, L.N. D'yachenko, et al., *Albedo and Angular Characteristics of Reflection from Underlying Surfaces and Clouds* (Gidrometeoizdat, Leningrad, 1981), 232 pp.